

NJC

Accepted Manuscript



This article can be cited before page numbers have been issued, to do this please use: F. P. Malan, E. Singleton, P. H. van Rooyen and M. Landman, *New J. Chem.*, 2019, DOI: 10.1039/C9NJ01220F.



This is an Accepted Manuscript, which has been through the Royal Society of Chemistry peer review process and has been accepted for publication.

Accepted Manuscripts are published online shortly after acceptance, before technical editing, formatting and proof reading. Using this free service, authors can make their results available to the community, in citable form, before we publish the edited article. We will replace this Accepted Manuscript with the edited and formatted Advance Article as soon as it is available.

You can find more information about Accepted Manuscripts in the [author guidelines](#).

Please note that technical editing may introduce minor changes to the text and/or graphics, which may alter content. The journal's standard [Terms & Conditions](#) and the ethical guidelines, outlined in our [author and reviewer resource centre](#), still apply. In no event shall the Royal Society of Chemistry be held responsible for any errors or omissions in this Accepted Manuscript or any consequences arising from the use of any information it contains.

Tandem transfer hydrogenation-epoxidation of ketone substrates catalysed by alkene-tethered Ru(II)-NHC complexes

Frederick P. Malan, Eric Singleton, Petrus H. van Rooyen, and Marilé Landman*

Abstract: A series of nine cyclopentadienyl Ru(II)-NHC complexes (**1-9**) have been synthesised by systematically varying the ligand and/or ligand substituents: η^5 -C₅H₄R' (R' = H, Me), EPh₃ (E = P, As), NHC (Im, Blm), where NHC = Im(R)(R') (R, R' = Me, Bn, 4-NO₂Bn, C₂H₄Ph, C₄H₇). Each of the Ru(II)-NHC complexes features an *N*-alkenyl tether to attain bidentate NHC ligands. All complexes found application as catalysts in the tandem transfer hydrogenation and epoxidation reactions of carbonyl substrates. The catalytic activity of the complexes was shown to be similar, with efficiencies of up to 69% conversion after 18 hours and varying alcohol:epoxide selectivity for a variety of electronically diverse carbonyl substrates. Complex **3**, with a nitro-containing substituent on the NHC ligand, was the only complex that showed preference for the alcohol product over the epoxide after 18 hours of reaction time.

Introduction

Alkene epoxidation is recognised as an important reaction in organic synthesis, able to provide enantiopure epoxides, which are important precursors in amongst other, drug synthesis.¹ However, non-atom-economical oxidants such as alkyl hydroperoxides and hypochlorites are often employed in catalytic epoxidation reactions.^{1(b)} Much less attention has been devoted to 'greener' oxygen-containing precursors, such as halohydrins. This is mainly because of the undesirable equilibrium that exists between the *vicinal* halohydrin and corresponding epoxide since the expelled mineral acid provides a nucleophilic halide to ring-open the formed epoxide. This problem could, however, be circumvented using acid scavengers or anion exchangers.¹ By making use of tandem hydrogenation and epoxidation reactions of the more readily available acyl halide precursors, a more efficient catalytic reaction is being devised. This would necessitate the use of highly versatile, transfer-hydrogenation active catalysts that withstands deactivation under oxidative, acidic conditions.²

During the last two decades an increasing amount of impetus has been placed on harnessing the synthetic and catalytic advantages that two independent research areas combine: Highly stabilising *N*-heterocyclic carbenes (NHCs), and the hemilability of multi-dentate hybrid ligand systems when coordinated to transition metals.³ NHCs constitute an ever-expanding ligand class capable of stabilising most transition metals in a range of different oxidation states.⁴⁻⁶ In addition, NHCs have been shown to act as 'smart' ligands, where their non-innocent, cooperative, switchable, and/or

multi-functional properties are exploited in addition to the tailored electronic and steric environments they provide.⁴ Bidentate NHCs introducing potentially hemilabile donor groups, enabling reversible dissociation from the metal centre, include phosphine,^{3(a), 3(f)} pyrimidine,⁷ ether,⁸ thioether,^{6(c)} carboxylate,^{6(c)} indenyl,⁹ oxazoline,¹⁰ amine,¹¹ and pyridine¹² moieties. However, the alkene functional group as secondary donor group received much less attention, despite it featuring in one of the first classical donor NHC complexes synthesised.^{3(d),13} To date, only Lavigne,^{3(c)} Bera^{2(c)} and Albrecht^{6(c)} have successfully employed alkene-tethered NHCs in the synthesis of a total of four ruthenium-NHC complexes (Figure 1) for application in catalysis studies.

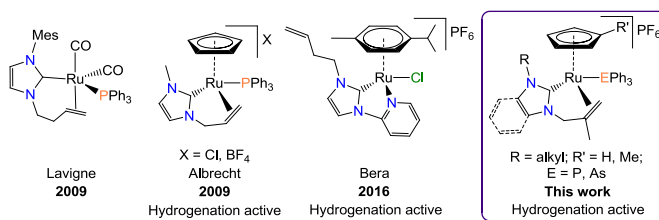


Figure 1. Previously reported alkene-functionalised Ru-NHC complexes, along with the new alkene-tethered Ru-NHC complexes of this study.

The lack of research on potentially hemilabile bidentate NHC ligands as part of half-sandwich ruthenium complexes, prompted us to investigate possible stability and catalytic enhancement effects that these chelating NHC ligands may provide. Half-sandwich ruthenium complexes containing NHC ligands are of special interest, given the rich synthetic and catalytic applications that they provide, especially with regard to transfer hydrogenation and epoxidation catalysis.^{2(c),3(e),14} Here we report the synthesis of nine new alkene-tethered half-sandwich Ru(II)-NHC complexes, evaluate their application in tandem transfer hydrogenation-epoxidation catalysis, and relate the respective catalytic activities in a DFT study.

Results and Discussion

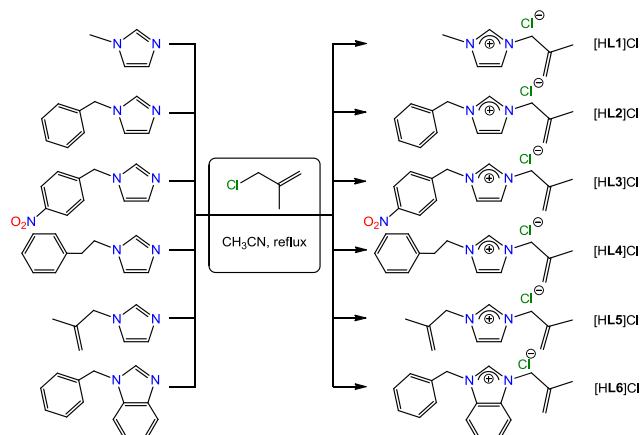
Synthesis of the NHC ligands and metal precursors

The NHC ligand precursors of this study were synthesised from *N*-substituted 3-chloro-2-methyl-propene imidazole (Scheme 1). Quaternisation reactions of the functionalised imidazole with the respective alkyl halides produce the corresponding alkene-tethered imidazolium chloride salts in excellent yields (94%, [HL1]Cl; 91%, [HL2]Cl; 67%, [HL3]Cl; 86%, [HL4]Cl; 88%, [HL5]Cl; 92%, [HL6]Cl). The purification of ligand precursors **L1-L6** entailed concentration of the crude reaction mixtures and washing with ethyl acetate to remove unreacted starting material. Removal of residual solvent *in vacuo* to resulted in the pure imidazolium salts

Department of Chemistry, University of Pretoria, 2 Lynnwood road, Hatfield, Pretoria, 0002, South Africa.
E-mail: marile.landman@up.ac.za

† Supporting information for this article is given via a link at the end of the document.

as white to light yellow crystalline solids or oils. The $^1\text{H-NMR}$ spectra of $[\text{H}(\text{L1-L6})]\text{Cl}$ all exhibited characteristic signals for the 2-methylpropenyl moiety: δ_{H} 1.39-1.73 ppm (singlet, methyl protons), 4.69-5.22 ppm (singlet, methylene protons), and 4.65-5.07 ppm (two singlets, alkene protons). The asymmetrical nature of the imidazolium salts resulted in two singlets for the imidazolium backbone protons at δ_{H} 6.66-7.81 ppm ($[\text{H}(\text{L1-L4})]\text{Cl}$, $[\text{HL6}]\text{Cl}$). The only symmetrical ligand precursor, $[\text{HL5}]\text{Cl}$ (Figure 2), exhibited one singlet at δ_{H} 7.38 ppm for these two protons. The acidic C(2)-H proton signals for the salts $[\text{H}(\text{L1-L6})]\text{Cl}$ varied between δ_{H} 9.40-10.82 ppm. The pseudo-carbenic C(2)-signals in the $^{13}\text{C-NMR}$



spectra ranges from 136.9 ($[\text{H}(\text{L2})]\text{Cl}$) to 144.3 ppm ($[\text{H}(\text{L6})]\text{Cl}$).

Scheme 1. Synthesis of ligand precursors $[\text{H}(\text{L1-L6})]\text{Cl}$ from the corresponding *N*-functionalised imidazoles.

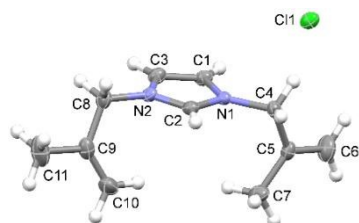
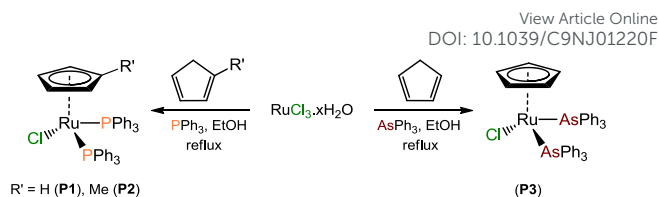


Figure 2. Perspective view of $[\text{HL5}]\text{Cl}$. Thermal ellipsoids are drawn at 50% level. The omission of one molecule of H_2O has been done for clarity purposes.

The half-sandwich precursors **P1-P3** were synthesised according to a modified version of the literature procedure (Scheme 2). In this modified procedure, an ethanolic solution of $\text{RuCl}_3 \cdot x\text{H}_2\text{O}$ is reacted with 2.5 equivalents of the respective pnictogen EPh_3 ($\text{E} = \text{P}, \text{As}$), and excess (> 2 equivalents) of the respective cyclopentadiene $\text{C}_5\text{H}_5\text{R}'$ ($\text{R}' = \text{H}, \text{Me}$). Reaction mixtures were allowed to heat under reflux overnight, which upon cooling allowed for the orange $[(\eta^5\text{-C}_5\text{H}_4\text{R}')\text{RuCl}(\text{EPh}_3)_2]$ ($\text{R}' = \text{H}, \text{Me}; \text{E} = \text{P}, \text{As}; \text{P1-P3}$) complexes to precipitate. The solid-state molecular structures of **P2**^{15(a)} and **P3** (Figure 3) are similar in that both assume the classical piano-stool structure with $\text{Ru1-Cg} = 1.844(3)$ (**P2**), $1.813(4)$ (**P3**) ($\text{Cg} =$ centroid of Cp ring); as well as $\text{Ru1-E1} = 2.3222(7)$ (**P2**, $\text{E} = \text{P}$), $2.4229(2)$ (**P3**, $\text{E} = \text{As}$). All of the Ru-Cg and Ru-E ($\text{E} = \text{P}, \text{As}$) bond lengths correspond well with related $\text{CpRuCl}(\text{PPh}_3)_2$ complexes.¹⁵



Scheme 2. Synthesis of the ruthenium(II) precursors **P1-P3**.

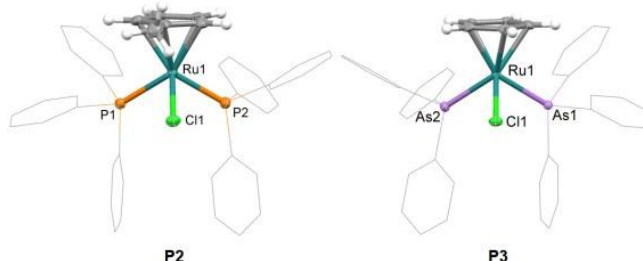
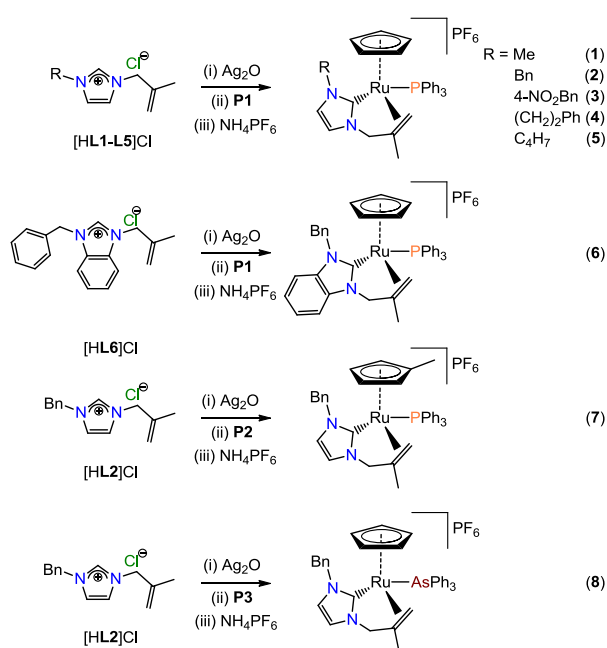


Figure 3. Perspective views of ruthenium precursors **P2** and **P3**. Thermal ellipsoids are drawn at 50% level. The phenyl moieties of the pnictogen moieties have been shown as wireframe presentations, as well as the omission of one molecule of CH_2Cl_2 within each structure have been done for clarity purposes.

Synthesis of the Ru(II)-NHC complexes

Each of the ligand precursors $[\text{H}(\text{L1-L6})]\text{Cl}$ contains an *N*-alkenyl substituent. After ruthenation of the ligand (**L1-L6**) by one of the precursors **P1-P3**, a normal (C2-substituted) NHC chelate complex (**1-8**) is formed in each case. Ruthenation was carried out using standard literature procedures^{2(c),6(c)} which involves reaction of the imidazolium salt with Ag_2O , with the exclusion of light. A biscarbene silver complex was formed, to which the appropriate half-sandwich ruthenium(II) precursor (**P1-P3**) was added *in situ*. Subsequent anion exchange with NH_4PF_6 in acetone yielded complexes **1-8** (Scheme 3). Complexes **1-6** resulted from the reaction of ligand precursors $[\text{H}(\text{L1-L6})]\text{Cl}$ with $[\text{CpRuCl}(\text{PPh}_3)_2]$ (**P1**), respectively, *via in situ* silver transmetalation. After purification, complexes **1-6** were obtained as air and light stable yellow to dark yellow solids. The yields of complexes **1-6** (after purification) were moderate (46-66%), with **3** being the lowest. The decreased reactivity of $[\text{HL3}]\text{Cl}$ is ascribed to the presence of an electron-withdrawing 4- NO_2Bn substituent on one of the N-atoms of the NHC ligand, which renders the ligand less donating than the others. Reactions of $[\text{HIm}(\text{Bn})(\text{C}_4\text{H}_7)]\text{Cl}$ (**L2** precursor) with $[(\eta^5\text{-C}_5\text{H}_4\text{R}')\text{RuCl}(\text{EPh}_3)_2]$ ($\text{R}' = \text{Me}, \text{E} = \text{P}, \text{P2}; \text{R}' = \text{H}, \text{E} = \text{As}, \text{P3}$) in a similar reaction procedure, yielded **7** (43 %, dark yellow solid) and **8** (62 %, brown solid), respectively. Spectroscopic evidence of NHC-coordination for **1-8** was obtained from their NMR spectra: Disappearance of the $^1\text{H-NMR}$ signal of $[\text{HL1-L6}]\text{Cl}$ corresponding to the C(2)-H proton between δ_{H} 9.40-10.82 ppm, along with the concomitant appearance of the $^{13}\text{C-NMR}$ carbene signal between δ_{C} 174.8-192.7 ppm were observed. $^1\text{H-NMR}$ signals for the cyclopentadienyl (**1-6, 8**) and methyl-cyclopentadienyl (**7**) moieties generally appeared in an equimolar ratio to the respective ligand **L1-L6**. Interestingly, other general NMR trends on comparing the imidazolium salts and the coordinated imidazolylidene ligands included upfield shifts of the *N*-alkyl signals, where for example shifts from δ_{H} 3.89 ppm (NMe, **L1**) to 2.94 ppm (**1**); 4.83 ppm (NCH₂, **L2**) to 4.71 ppm (**2**), and 4.91 ppm (NCH₂, **L5**) to 3.59 ppm (**5**), have been observed.

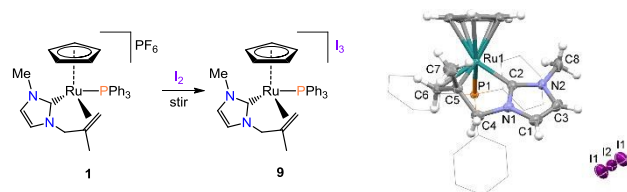


Scheme 3. Syntheses of complexes **1-8** from the respective Ru(II) precursors **P1-P3**, and ligand precursors [H(L1-L6)]Cl.

In addition, upfield shifts of the C(4)-H and C(5)-H protons in **L1-L5** after complexation have been observed, with the shift of **L1** being the most notable: an upfield shift occurs from δ_{H} 7.74 and 7.81 ppm (**L1**) to 6.92 and 7.03 ppm (**1**) respectively. This is indicative of a significant degree of electron density perturbation on the C(4) and C(5) carbon atoms after complexation due to higher electron density on the C(2) position.² The signal relating to the PPh₃ ligand in the ³¹P-NMR spectra of complexes **1-7** was observed in a narrow region between δ_{P} 56.5-58.1 ppm. ¹H-NMR signals for the alkenyl moiety were in general very similar for complexes **1-8**: the methyl protons resonated between δ_{H} 1.74-2.18 (s) ppm, the unsymmetrical alkene protons between δ_{H} 1.89-2.51 (d, ³J_{HP} = 15 Hz) and 3.73-4.28 (s) ppm, and the methylene protons between δ_{H} 1.13-2.08 (d, ²J_{HH} = 12 Hz) and 3.51-4.00 (d, ²J_{HH} = 12 Hz) ppm. In complex **5**, containing both free and bound *N*-alkenyl moieties, signals pertaining to the bound tether were observed more upfield (2.07 and 3.85 for =CH₂ protons) as compared to the free tether (4.50 and 4.97 for =CH₂ protons), which has little to no interaction with the metal centre.

A slight degree of fluxionality of the alkenyl tether of complexes **1-8** was inferred from the variable temperature ¹H-NMR spectra of **4** (bearing both a coordinated alkenyl tether, as well as a free phenethyl *N*-substituent). The variable temperature ¹H-NMR

spectra were obtained from a (CD₃)₂CO solution containing **4** and recorded between -50°C and +50°C (Supplementary Information). In the higher temperature spectra (> 20°C), decoalescence is observed only for the multiplet at 3.02 ppm, assigned to the ethylene linker protons of the phenethyl substituent, in the -50°C spectrum into two multiplets at 2.93 and 3.09 ppm. No coalescence is seen for the signals related to the alkenyl tether. The signals related to the alkenyl tether only underwent an upfield shift of *ca.* 0.48 ppm (d, ²J_{HH} = 12 Hz, NCH₂ protons) and 0.19 ppm (d, ²J_{HH} = 15 Hz, =CH₂ protons) at low temperatures. In an attempt to further probe the hemilability and subsequent reactivity of the *N*-alkenyl moiety, C=C bond cleavage *via* halogenation was attempted. Reaction of a DCM solution of **1** with a slight excess of I₂ resulted in an anion exchange with PF₆⁻ to form the complex [CpRu(PPh₃){Im(Me)(C₄H₇)}]I₃ (**9**, Scheme 4). The presence of minute amounts of moisture is thought to have mediated a reversible disproportionation reaction between I₂ and H₂O.^{16(a),16(b)} Furthermore, no reaction was observed after heating the sample for several hours. This indicates a level of robustness in the Ru-alkene bond, and hence a lower degree of hemilability that exists in solution than originally anticipated.



Scheme 4. Reaction of **1** with I₂ to form **9**. Inset: Perspective view of **9**. Thermal ellipsoids are drawn at 50% level. The phenyl moieties of PPh₃ have been shown as wireframe presentations for clarity purposes.

The proposed molecular structures of the novel Ru-NHC complexes were supported by single crystal X-ray diffraction (SCXRD) studies. C(2)-carbene coordination for complexes **1**, **2**, **4**, **5**, **8** and **9** were confirmed (Scheme 4, Figure 4). All of the half-sandwich Ru(II) complexes assumed pseudo three-legged piano stool structures, where the η²-alkene moiety is considered as one leg.^{2(c),6(c)} Selected bond lengths and angles are summarised in Table S4 in the Supplementary Information. If chelation of the alkene-tether in complexes **1-4** is considered to form pseudo-five membered ruthenacycles, the resulting acute bite angles are almost identical for all complexes, and varies between 89.38(1)° (**8**) and 89.71(1)° (**4**). While the tether and imidazolium planes are essentially coplanar in related five-membered metallacycles,^{6(c)} the alkene-containing complexes exhibit anticlinal torsion angles (between the alkene and imidazolylidene mean plane) of either between 24.7(3)° and 28.3(3)° (**1**, **2**, **4**, **5**), or -22.6(7)° (**8**) and -26.8(3)° (**9**).

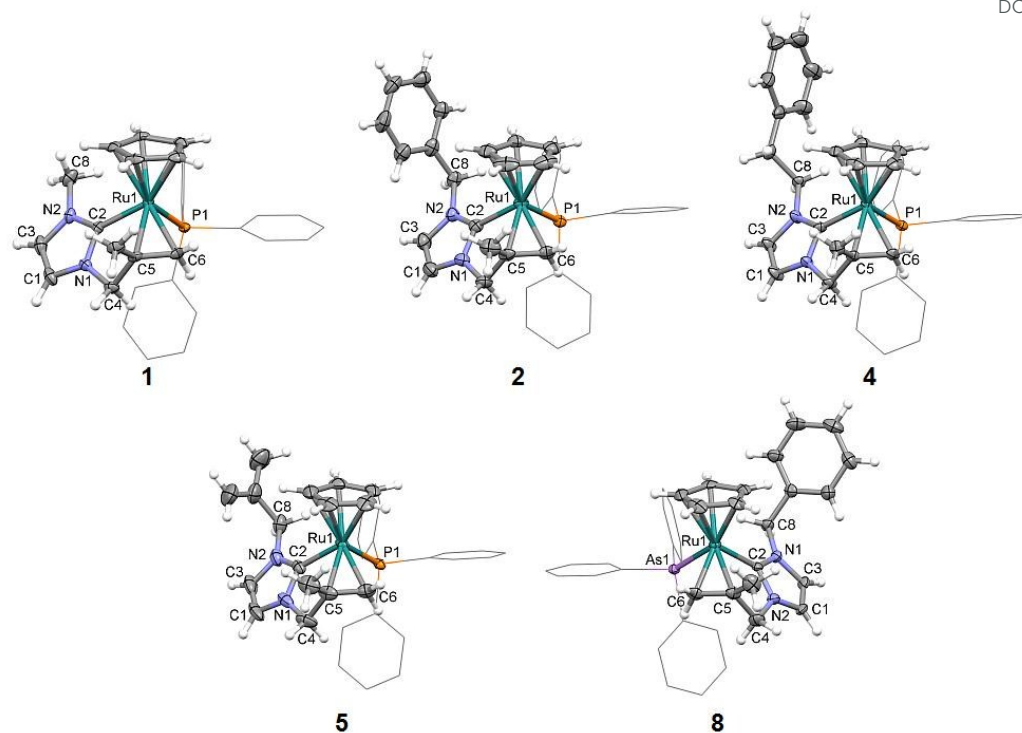


Figure 4. Perspective views of Ru(II)-NHC complexes **1**, **2**, **4**, **5**, and **8**. Thermal ellipsoids are drawn at 50% level. For clarity purposes, the phenyl moieties of the pnictogen moieties have been shown as wireframe presentations, as well as the omission of one molecule of PF_5 within each structure, including the omission of one molecule of CH_2Cl_2 (**2** and **8**).

It is also interesting to note that the Ru-C(2) bond distances of the complexes have a narrow distribution which fall between 2.033(2) Å (**1**) and 2.042(2) Å (**2**). This is indicative of the negligible electronic effect the different NHC ligands have on the Ru-NHC bond. However, the Ru-C bond distances are in good agreement with similar Ru-C bond distances of related normally bound Ru(II)-NHC complexes.^{6(c),14(a),15}

Catalysis Studies

The ability of catalysts to mediate tandem reactions are highly attractive since multistep transformations allow for the minimisation of follow-up batch reactions, employment of less catalyst(s), and a rapid increase in molecular complexity from readily available starting materials.^{16(c)} Transfer hydrogenation in particular has been widely studied by numerous groups over the years, although the added benefits of employing metal-NHC complexes as catalysts were only realised in the last two decades.^{2(a)} Very few studies have been concerned with the one-pot functionalisation of post-hydrogenation products.

We were therefore interested in the base-mediated epoxidation of the formed halohydrins as a secondary reaction. Similar to numerous other reported half-sandwich Ru(II) complexes,^{12,17} **1-8** were all found to be transfer hydrogenation active. Standard conditions were employed, *i.e.* excess isopropanol as a hydrogen donor, base (KOH or KO^tBu) as activator, and 4'-bromophenacyl bromide (BPAB) as substrate. ¹H-NMR analyses on reaction

mixtures in the presence of anisole (internal standard) taken over a period of 18 hours, suggested a tandem reaction, whereby a mixture of secondary alcohol (halohydrin) and the ring-closed epoxide products were observed. No induction time was observed for all reactions under optimised conditions.

All complexes except **3** showed similar activity (Table 1), with initial TOFs of 8-12 h⁻¹ (total conversion) were observed (determined after the first 15 minutes reaction time), under typical conditions. The latter TOFs compare poorly with some of the best-performing half-sandwich ruthenium-based catalysts,^{17(a),18} where TOFs of up to 3000 h⁻¹ have been reported for transfer hydrogenation catalysis. However, the TOFs of **1-8** fall within the lower range of related half-sandwich bidentate NHC-Ru(II) analogues.^{12,17} A change of pnictogen ligand (As vs. P) has very little effect on the catalytic activity (compare entry 2 with entry 8 in Table 1). Chelation generally stabilises catalysts to render them more robust and therefore less prone to catalyst deactivation by means of catalyst poisons. However, chelation may also inhibit fast substrate conversion through the occupation of required vacant sites, and hence could reduce the overall yield.¹⁹ This effect might be prevalent in the catalytic activities of **1-8**, where a slow transfer hydrogenation reaction of BPAB occurs during the initial few hours of reaction, followed by the concomitant epoxidation reaction of the alcohol intermediate product.

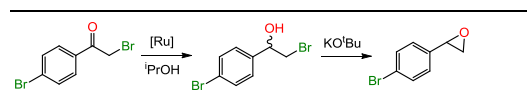
After reaction optimisation (Table S5 in the Supplementary Information), complexes **1-8** were screened for their catalytic activity. After two hours' reaction time, complexes **1**, **2**, **4**, **5**, and **7** all exhibited comparable activity, having converted between 27%

(5) and 34% (1) of the substrate. Complex 3, bearing the *N*-4-NO₂-benzyl NHC ligand, fared the worst, with a conversion of 23% (TOF₁₅ = 4 h⁻¹). The efficiency of the transfer hydrogenation-epoxidation reaction was found to be temperature and base-dependent. At room temperature, the reaction proceeds sluggishly (9% conversion after 18 hours). Without addition of a base, low (< 31%) conversions were obtained. Furthermore, the low conversions obtained when using KOH (31% after 6h) as base necessitated the use of the stronger KO^tBu base, for which better conversions were obtained (56% after 6 hours).

In general, it is seen that similar *N*-substituents (methyl, benzyl, phenethyl) on the NHC ligand have little effect on the catalytic activity (entries 1, 2 and 4). The lower conversion of complex 5 is attributed to the second *N*-alkenyl group on the NHC ligand: the presence of a potential chelating group competes with substrate coordination once an available site on the ruthenium centre is generated. Although comparable catalytic activities (within a 3% error range) have been observed for complexes 1-8, these result appear to indicate that steric effects may play a role in reducing the reaction rate, especially if an inner sphere mechanism is considered. Both the *N*-substituent and the backbone moiety of the NHC ligand may contribute to the overall steric bulk of the resulting Ru-NHC complex, for which complex 1 (*N*-Me) is sterically less demanding than 4 (*N*-(CH₂)₂Ph) or 6 (benzimidazole vs. imidazole). The resulting effect is seen in the final substrate conversions observed (60% (1) vs. 55% (4) and 51% (6)). Electronic properties of the substrate marginally affected the conversions (Table 2), *i.e.* more electron-donating substituents (4'-Me vs. 4'-Br; entry 2) resulted in slightly higher conversions (69% (Me, entry 2, Table 2) vs. 62% (Br, entry 8, Table 1)). The substrates with 4'-OH and 4'-NH₂ groups showed lower conversion, probably due to coordination interferences. The presence of the electron-withdrawing moieties (Br, NO₂) appears to deactivate the carbonyl moiety due to resonance effects.

A lack of selectivity is observed in the catalytic conversions using complexes 1-8. The selectivity between the halohydrin and corresponding epoxide is shifted towards the halohydrin during the initial two hours' reaction time (69-84%(alcohol):17-31%(epoxide)). After six hours' reaction time, near equimolar amounts of the halohydrin and corresponding epoxide are observed (48-61%(alcohol):39-52%(epoxide)). A shift towards the formed epoxide is observed after 18 hours' reaction time (27-43%(alcohol):57-73%(epoxide)). This shift is more pronounced for substrates with electron-withdrawing substituents (NO₂, 22%(alcohol):78%(epoxide)) where the corresponding epoxide is more readily formed after a slow(er) transfer hydrogenation step.

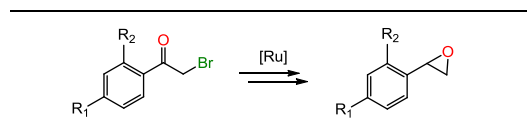
Table 1. Tandem transfer hydrogenation-epoxidation of BPAB using 1-8 as catalyst.



Entry	Complex	Conversion ^a (%)			Selectivity ^b (%, alc:epox)
		2h	6h	18h	
1	1	34	52	60	35:65
2	2	32	48	58	43:57
3	3	23	36	39	62:38
4	4	33	49	55	40:60
5	5	27	43	45	38:62
6	6	26	46	51	29:71
7	7	29	48	52	38:62
8	8	37	56	62	27:73

General conditions: 4'-bromophenyl bromide (BPAB, 0.6 mmol), ⁱPrOH (4 mL), base (1.2 eq.), anisole as internal standard (65 μL, 0.6 mmol), [Ru] (2 mol%), 110 °C. ^a Determined by ¹H-NMR, based on the average of at least two runs. ^b Selectivity (%): alc:epox = alcohol:epoxide.

Table 2. Substrate screening in the tandem transfer hydrogenation-epoxidation.



Entry	R ₁	R ₂	Conversion ^a (%)			Selectivity ^b (%, alc:epox)
			2h	6h	18h	
1	H	H	29	49	56	41:59
2	Me	H	32	55	69	36:64
3	H	OH	24	38	48	39:61
4	NH ₂	H	19	31	41	34:66
5	NO ₂	H	20	28	36	22:78

General conditions: substrate (0.6 mmol), ⁱPrOH (4 mL), KO^tBu (1.2 eq.), anisole (65 μL, 0.6 mmol), 8 (2 mol%), 110 °C.

^a Determined by ¹H-NMR, based on the average of at least two runs. ^b Selectivity (%): alc:epox = alcohol:epoxide.

A mechanism for the tandem transformation is proposed in Figure 5, using complex **8**. Analogous to similar CpRu derivatives, it is reasonable to assume that catalytic transfer hydrogenation occurs *via* a classic monohydride mechanism.^{17(b)} Dissociation of an AsPh₃ ligand (a) allows for isopropoxide coordination (b), which subsequently dissociates as acetone after β -hydride elimination. The latter process leads to the formation of the active hydride species (c) needed for hydrogen transfer. By reversible alkene dissociation, an additional vacant site is created by which an incoming carbonyl substrate (d) is reduced to the alkoxide-moiety (e) by means of hydrogen transfer. The functionalised alkoxide intermediate is then substituted for isopropoxide (f). Finally, a tandem intramolecular nucleophilic attack of the oxo-group of the deprotonated halohydrin occurs to eliminate a bromido anion, along with the desired epoxide (g).

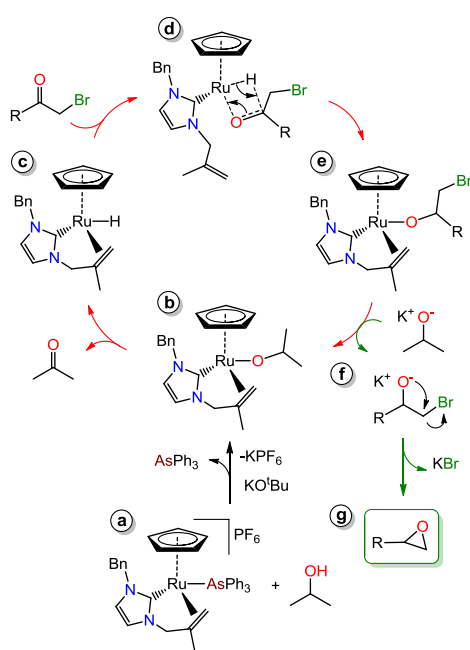


Figure 5. Proposed mechanism for the tandem transfer hydrogenation and epoxidation transformation reaction.

DFT studies

In order to probe the stability, reactivity and subsequent catalytic applicability of complexes **1-8**, a DFT study of the frontier orbitals is presented (Figure 6). In Figure 6 the HOMO and LUMO representations, the energies of the HOMO and LUMO, as well as the corresponding energy gap (energy difference between the HOMO and LUMO) of all complexes are presented. In terms of the molecular orbitals, similarities among complexes **1-8** could be drawn: Precursor complexes **P1-P3** all exhibit a LUMO distributed mainly over the ruthenium centre with a minor contribution from the cyclopentadienyl ligand. The HOMO of **P1-P3** is uniquely positioned mainly on the pnictogen moieties. After NHC-functionalisation, electron density within complexes **1-8** is shifted

such that the LUMO is distributed over the ruthenium and NHC ligand. This might be indicative of the Ru-NHC bond being prone to reduction, especially in the presence of harsh reducing conditions. In contrast, the HOMO of all the complexes except complex **3** exhibit ruthenium and pnictogen character. The HOMO of complex **3** is exclusively positioned over the 4-NO₂-benzyl moiety of the NHC ligand. This may suggest that a further oxidation process could involve this moiety.

Upon reaction of **P1**, **P2** or **P3** with the respective NHC ligands, the corresponding HOMO and LUMO energies of **1-8** are lowered. This is indicative of the stabilisation effect the chelating NHC exerts on the resulting complex. Furthermore, the energy gaps of all complexes except **3** are larger by around 0.34-0.57 eV. The smallest energy gap of 3.25 eV (**3**) corresponds to the least stable (and more reactive) complex of complexes **1-8**. This observation corresponds to the experimental catalytic activities of complexes **1-8**.²⁰ Complex **3** being the least active catalyst, exhibits the smallest energy gap, is the least stable, and is therefore the most susceptible to fast catalyst deactivation. The energy gaps of the remainder of the complexes (4.31-4.55 eV) are comparable, and correspond to similar catalytic activities observed for these complexes.

Relating to the Principle of Maximum Hardness (PMH) with respect to molecular orbital (MO) theory, the hardness of a molecule (η) is defined as half the energy gap between the HOMO and the LUMO of that molecule.^{20(b)} A chemical system therefore is inclined to maximise the hardness of its respective molecules since a hard molecule tends to have a large(r) energy gap.^{20(b)} Comparing the hardness of complexes **1-8**, all complexes ($2.16 \leq \eta \leq 2.27$) except complex **3** ($\eta = 1.63$) exhibit relatively hard character, and are therefore more robust against catalyst deactivation than complex **3**.

Conclusions

Variation of the *N*-alkyl group of the NHC, the ancillary pnictogen ligand, and (substituted) cyclopentadienyl ligand, provided access to eight unique half-sandwich Ru(II)-NHC complexes. The NHC ligands of these complexes were tailored to feature an alkenyl-group to act as a hemi-labile group for catalysis purposes. Catalytic studies involving the tandem transfer hydrogenation and epoxidation of a range of electronically diverse phenacyl bromides suggest a low degree of hemilability provided by the alkenyl-tether. The catalytic activities of complexes **1-8** were found to be similar while selectivities favoured the epoxide product. The only exception was complex **3**, which favoured halohydrin formation after 18 hours' reaction time (62:38 alc:epox). Furthermore, a slight deactivating effect has been observed for the phenacyl bromide substrates bearing electron-withdrawing moieties.

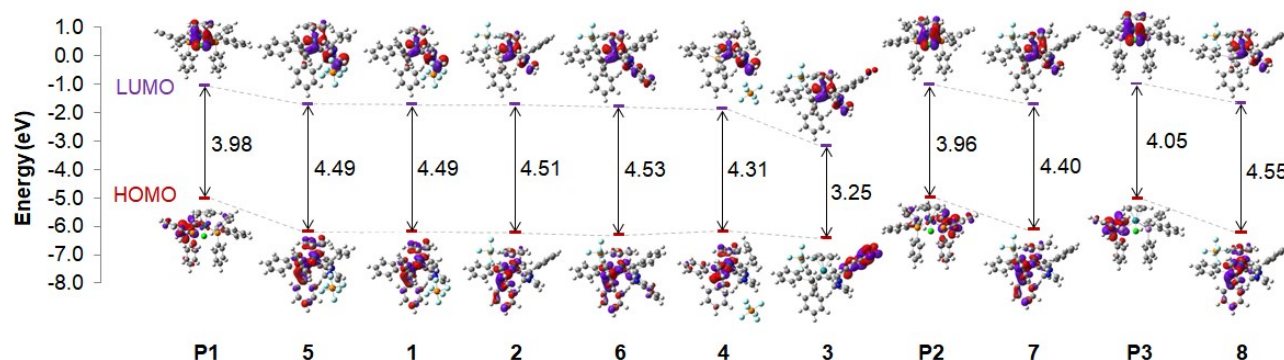


Figure 6. Frontier orbitals of the precursor complexes P1-P3, and CpRu-NHC complexes 1-8. Representations are ordered according to descending LUMO energy (1-8) from the respective precursor (P1-P3)

However, enhanced selectivities towards the epoxide product were observed for the latter substrates.

chromatography, using gradient elution with Et₂O/CH₂Cl₂. Yellow to dark-yellow solids were obtained.

Experimental Section

General Procedures

All experiments were carried out under an argon atmosphere using standard Schlenk techniques. Solvents were dried and distilled from appropriate drying agents prior to use. The new imidazolium chloride ligands [H(L1-L6)]Cl, as well as the metal precursors [CpRuCl(PPh₃)₂] (**P1**), [MeCpRuCl(PPh₃)₂] (**P2**), and [CpRuCl(AsPh₃)₂] (**P3**) were synthesised and purified according to standard literature procedures. All other chemicals were purchased from commercial suppliers and used without further purification. ¹H (300 MHz) and ¹³C{¹H} (76 MHz) NMR spectra were recorded on a Bruker Avance-400 spectrometer using CDCl₃. All measurements were performed at ambient temperature (298 K), unless otherwise noted. Chemical shifts were referenced to the internal residual solvent resonances. Microanalytical analyses (%CHNS) were obtained using a Thermo Scientific Flash 2000 elemental analyser fitted with a TCD detector. Electrospray mass spectra (ESI-MS) were recorded on a MicromassQuatro LC instrument.

General synthesis of half-sandwich Ru(II)-NHC complexes (1-8):

A suspension of the appropriate imidazolium chloride salt (4 mmol) in CH₂Cl₂ (30 mL) containing Ag₂O (0.93 g, 4 mmol) was stirred at 30°C for 12 hours in the absence of light. The mixture was filtered to which the appropriate half-sandwich Ru(II) precursor ([CpRuCl(PPh₃)₂] **P1**, [MeCpRuCl(PPh₃)₂] **P2**, or [CpRuCl(AsPh₃)₂] **P3**, 4 mmol) was added and heated under reflux for 36 hours. The crude reaction mixture was filtered, concentrated *in vacuo* (5 mL), to which acetone (15 mL), and NH₄PF₆ (0.65 g, 4 mmol) was added. The reaction mixture was stirred for a further hour after which the mixture was evaporated *in vacuo*, and purified by silica gel column

[CpRu(PPh₃)(L1)]PF₆ (**1**): Yield: 66%. ¹H NMR (CDCl₃): δ_H = 1.14 (d, ²J_{HH} = 12 Hz, 1H, NCH₂), 1.75 (s, 3H, CCH₃), 1.89 (d, ³J_{HP} = 15 Hz, 1H, =CCH₂), 2.94 (s, 3H, NCH₃), 3.52 (d, ²J_{HH} = 12 Hz, 1H, NCH₂), 3.76 (s, 1H, =CCH₂), 5.03 (s, 5H, C₅H₅), 6.92 (s, 1H, C_{imi}H), 7.03 (s, 1H, C_{imi}H), 7.21-7.38 (m, 15H, H_{Ph}). ¹³C{¹H} NMR (CD₃CN): δ_C = 32.7 (s, CCH₃), 37.8 (s, NCH₃), 48.2 (s, =CCH₂), 57.5 (s, NCH₂), 81.1 (s, =CCH₂), 88.7 (s, C₅H₅), 118.3 (s, C_{imi}H), 121.4 (s, C_{imi}H), 126.0 (s, C_{Ph}), 129.5 (s, C_{Ph}), 131.4 (s, C_{Ph}), 134.4 (s, *ipso* C_{Ph}), 175.8 (s, C-Ru). ³¹P{¹H} NMR (CDCl₃): δ_P = -144.1 (septet, ¹J_{PF} = 704 Hz, PF₆), 58.1 (s, PPh₃). CHN found (calcd) for [C₃₁H₃₂F₆N₂P₂Ru]×0.5C₃H₆O: C, 53.17 (52.85), H, 4.71 (4.78), N, 3.93 (3.79)%. HR-MS (ESI): m/z 565.1344 (1⁺) calcd for C₃₁H₃₂N₂PRu 565.1347.

[CpRu(PPh₃)(L2)]PF₆ (**2**): Yield: 58%. ¹H NMR (CDCl₃): δ_H = 1.54 (d, ²J_{HH} = 12 Hz, 1H, NCH₂), 1.91 (s, 3H, CCH₃), 2.08 (d, ³J_{HP} = 15 Hz, 1H, =CCH₂), 3.71 (d, ²J_{HH} = 12 Hz, 1H, NCH₂), 3.88 (s, 1H, =CCH₂), 4.71 (s, 2H, NCH₂), 4.87 (s, 5H, C₅H₅), 6.94 (s, 1H, C_{imi}H), 6.96 (s, 1H, C_{imi}H), 6.96-7.07 (m, 5H, H_{Ph}), 7.19-7.44 (m, 15H, H_{Ph}). ¹³C{¹H} NMR (CDCl₃): δ_C = 32.8 (s, CCH₃), 48.4 (s, =CCH₂), 57.0 (s, NCH₂), 65.8 (s, NCH₂), 82.4 (s, =CCH₂), 87.5 (s, C₅H₅), 126.1 (s, C_{imi}H), 127.9 (s, C_{imi}H), 128.2 (s, C_{Ph}), 128.8 (s, C_{Ph}), 128.9 (s, C_{Ph}), 129.1 (s, C_{Ph}), 129.9 (s, C_{Ph}), 133.3 (s, C_{Ph}), 133.5 (s, *ipso* C_{Ph}), 133.7 (s, *ipso* C_{Ph}), 176.0 (s, C-Ru). ³¹P{¹H} NMR (CDCl₃): δ_P = -144.2 (septet, ¹J_{PF} = 713 Hz, PF₆), 57.5 (s, PPh₃). CHN found (calcd) for [C₃₇H₃₆F₆N₂P₂Ru]×0.5CH₂Cl₂: C, 54.54 (54.39), H, 4.42 (4.50), N, 3.17 (3.38)%. HR-MS (ESI): m/z 641.1656 (2⁺) calcd for C₃₇H₃₆N₂PRu 641.1660.

[CpRu(PPh₃)(L3)]PF₆ (**3**): Yield: 46%. ¹H NMR (CDCl₃): δ_H = 1.82 (d, ²J_{HH} = 12 Hz, 1H, NCH₂), 2.18 (s, 3H, CCH₃), 2.36 (d, ³J_{HP} = 15 Hz, 1H, =CCH₂), 3.98 (d, ²J_{HH} = 12 Hz, 1H, NCH₂), 4.28 (s, 1H, =CCH₂), 5.25 (s, 5H, C₅H₅), 5.61 (s, 2H, NCH₂), 6.88 (s, 1H, C_{imi}H), 6.90 (s, 1H, C_{imi}H), 6.93-7.16 (m, 4H, H_{Ph}), 7.26-7.32 (m, 9H, H_{Ph}), 7.69 (s, 2H, H_{Ph}), 8.12 (m, 4H, H_{Ph}). ¹³C{¹H} NMR (CDCl₃): δ_C = 34.3 (s, CCH₃), 49.9 (s, =CCH₂), 57.6 (s, NCH₂), 59.6 (s, NCH₂), 81.6 (s, =CCH₂), 87.5 (s, C₅H₅), 119.7 (s, C_{imi}H), 123.9 (s, C_{imi}H), 128.2 (s, C_{Ph}), 128.6 (s, C_{Ph}), 129.0 (s, C_{Ph}),

130.0 (s, C_{Ph}), 130.5 (s, C_{Ph}), 133.8 (s, C_{Ph}), 137.3 (s, *ipso* C_{Ph}), 143.3 (s, *ipso* C_{Ph}), 178.2 (s, C-Ru). ³¹P{¹H} NMR (CDCl₃): δ_P = -144.2 (septet, ¹J_{PF} = 716 Hz, PF₆), 57.2 (s, PPh₃). CHN found (calcd) for [C₃₇H₃₅F₆N₃O₂P₂Ru]×0.5H₂O: C, 52.95 (52.92), H, 4.55 (4.32), N, 5.03 (5.00)%. HR-MS (ESI): m/z 686.1208 (**3**⁺) calcd for C₃₇H₃₅N₃O₂PRu 686.1510.

[CpRu(PPh₃)(L4)]PF₆ (**4**): Yield: 55%. ¹H NMR ((CD₃)₂CO): δ_H = 1.60 (d, ²J_{HH} = 12 Hz, 1H, NCH₂), 1.95 (s, 3H, CCH₃), 2.15 (d, ³J_{HP} = 15 Hz, 1H, CH₂), 3.07 (dddd, ³J_{HH} = 6, 10, 14, 36 Hz, 2H, NCH₂CH₂), 3.67 (dddd, ³J_{HH} = 6, 10, 14, 77 Hz, 2H, NCH₂CH₂), 3.85 (d, ³J_{HH} = 12 Hz, 1H, NCH₂), 4.03 (s, 1H, =CCH₂), 5.27 (s, 5H, C₅H₅), 7.06 (s, 1H, C_{imi}H), 7.08 (s, 1H, C_{imi}H), 7.10-7.24 (m, 5H, H_{Ph}), 7.25-7.57 (m, 15H, H_{Ph}). ¹³C{¹H} NMR (CDCl₃): δ_C = 32.8 (s, CCH₃), 48.3 (s, =CCH₂), 50.9 (s, NCH₂CH₂), 56.8 (s, NCH₂), 65.8 (s, NCH₂CH₂), 82.4 (s, =CCH₂), 87.5 (s, C₅H₅), 121.3 (s, C_{imi}H), 122.9 (s, C_{imi}H), 128.4 (s, C_{Ph}), 128.8 (s, C_{Ph}), 129.0 (s, C_{Ph}), 130.5 (s, C_{Ph}), 131.4 (s, C_{Ph}), 133.4 (s, C_{Ph}), 133.9 (s, *ipso* C_{Ph}), 137.0 (s, *ipso* C_{Ph}), 174.7 (s, C-Ru). ³¹P{¹H} NMR (CDCl₃): δ_P = -144.2 (septet, ¹J_{PF} = 713 Hz, PF₆), 57.4 (s, PPh₃). CHN found (calcd) for [C₃₈H₃₈F₆N₂P₂Ru]×0.5CH₂Cl₂: C, 54.59 (54.91), H, 4.40 (4.67), N, 3.15 (3.33)%. HR-MS (ESI): m/z 655.1877 (**4**⁺) calcd for C₃₈H₃₈N₂PRu 655.1816.

[CpRu(PPh₃)(L5)]PF₆ (**5**): Yield: 61%. ¹H NMR (CDCl₃): δ_H = 1.53 (d, ²J_{HH} = 12 Hz, 1H, NCH₂), 1.54 (s, 3H, CCH₃), 1.91 (s, 3H, CCH₃), 2.07 (d, ³J_{HP} = 15 Hz, 1H, =CCH₂), 3.59 (m, 2H, NCH₂), 3.69 (d, ²J_{HH} = 12 Hz, 1H, NCH₂), 3.85 (s, 1H, =CCH₂), 4.50 (s, 1H, =CCH₂), 4.98 (s, 1H, =CCH₂), 5.00 (s, 5H, C₅H₅), 7.08 (s, 1H, C_{imi}H), 7.10 (s, 1H, C_{imi}H), 7.37-7.67 (m, 15H, H_{Ph}). ¹³C{¹H} NMR (CDCl₃): δ_C = 30.9 (s, CCH₃), 32.9 (s, CCH₃), 48.9 (s, =CCH₂), 55.0 (s, =CCH₂), 57.0 (s, NCH₂), 65.8 (s, NCH₂), 79.9 (s, =CCH₂), 82.5 (s, =CCH₂), 87.6 (s, C₅H₅), 121.0 (s, C_{imi}H), 124.6 (s, C_{imi}H), 128.4 (s, C_{Ph}), 130.8 (s, C_{Ph}), 131.9 (s, C_{Ph}), 140.8 (s, *ipso* C_{Ph}), 175.6 (s, C-Ru). ³¹P{¹H} NMR (CDCl₃): δ_P = -144.3 (septet, ¹J_{PF} = 713 Hz, PF₆), 57.5 (s, PPh₃). CHN found (calcd) for [C₃₄H₃₆F₆N₂P₂Ru]×0.25CH₂Cl₂: C, 53.70 (53.36), H, 4.59 (4.77), N, 3.63 (3.66)%. HR-MS (ESI): m/z 605.1715 (**5**⁺) calcd for C₃₄H₃₆N₂PRu 605.1660.

[CpRu(PPh₃)(L6)]PF₆ (**6**): Yield: 51%. ¹H NMR (CDCl₃): δ_H = 1.67 (d, ²J_{HH} = 12 Hz, 1H, NCH₂), 2.01 (s, 3H, CCH₃), 2.23 (d, ³J_{HP} = 15 Hz, 1H, =CCH₂), 4.00 (d, ²J_{HH} = 12 Hz, 1H, NCH₂), 4.07 (s, 1H, =CCH₂), 4.67 (s, 2H, NCH₂), 4.93 (s, 5H, C₅H₅), 7.21-7.24 (m, 4H, H_{Ph}), 7.34-7.37 (m, 4H, H_{Ph}), 7.41-7.46 (m, 12H, H_{Ph}), 7.52 (m, 2H, H_{Ph}), 7.61-7.66 (m, 3H, H_{Ph}). ¹³C{¹H} NMR (CDCl₃): δ_C = 30.9 (s, CCH₃), 49.0 (s, =CCH₂), 50.7 (s, NCH₂), 54.4 (s, NCH₂), 80.6 (s, =CCH₂), 88.2 (s, C₅H₅), 125.0 (s, C_{imi}H), 126.9 (s, C_{imi}H), 128.0 (s, C_{imi}H), 128.4 (s, C_{Ph}), 128.5 (s, C_{imi}H), 128.9 (s, C_{Ph}), 129.4 (s, C_{Ph}), 130.5 (s, C_{Ph}), 131.9 (s, C_{Ph}), 132.1 (s, C_{Ph}), 133.6 (s, *ipso* C_{Ph}), 133.7 (s, *ipso* C_{Ph}), 192.7 (s, C-Ru). ³¹P{¹H} NMR (CDCl₃): δ_P = -144.2 (septet, ¹J_{PF} = 713 Hz, PF₆), 56.5 (s, PPh₃). CHN found (calcd) for [C₄₁H₃₈F₆N₂P₂Ru]×0.9CH₂Cl₂: C, 55.19 (55.26), H, 4.25 (4.40), N, 2.95 (3.08)%. HR-MS (ESI): m/z 691.1312 (**6**⁺) calcd for C₄₁H₃₈N₂PRu 691.1816.

[MeCpRu(PPh₃)(L2)]PF₆ (**7**): Yield: 43%. ¹H NMR (CDCl₃): δ_H = 1.50 (d, ²J_{HH} = 12 Hz, 1H, NCH₂), 1.90 (s, 3H, CCH₃), 1.94 (s, 3H, C₅H₄CH₃),

2.51 (d, ³J_{HP} = 15 Hz, 1H, =CCH₂), 3.72 (d, ²J_{HH} = 12 Hz, 1H, NCH₂), 4.18 (s, 1H, =CCH₂), 4.36 (d, ²J_{HH} = 8 Hz, 2H, NCH₂), 4.82 (s, 2H, C₅H₄CH₃), 5.00 (s, 2H, C₅H₄CH₃), 6.81 (s, 1H, C_{imi}H), 6.82 (s, 1H, C_{imi}H), 6.82-7.00 (m, 5H, H_{Ph}), 7.14-7.45 (m, 15H, H_{Ph}). ¹³C{¹H} NMR (CDCl₃): δ_C = 12.2 (s, C₅H₄CH₃), 33.3 (s, CCH₃), 53.3 (s, =CCH₂), 56.9 (s, NCH₂), 57.7 (s, NCH₂), 78.3 (s, C₅H₄CH₃), 80.3 (s, =CCH₂), 87.9 (s, C₅H₄CH₃), 101.5 (s, C₅H₄CH₃), 121.2 (s, C_{imi}H), 124.7 (s, C_{imi}H), 128.1 (s, C_{Ph}), 128.8 (s, C_{Ph}), 129.0 (s, C_{Ph}), 129.2 (s, C_{Ph}), 130.8 (s, C_{Ph}), 133.5 (s, C_{Ph}), 133.7 (s, *ipso* C_{Ph}), 135.8 (s, *ipso* C_{Ph}), 176.1 (s, C-Ru). ³¹P{¹H} NMR (CDCl₃): δ_P = -144.2 (septet, ¹J_{PF} = 713 Hz, PF₆), 58.1 (s, PPh₃). CHN found (calcd) for [C₃₈H₃₈F₆N₂P₂Ru]×0.7CH₂Cl₂: C, 54.06 (54.23), H, 4.51 (4.63), N, 3.49 (3.27)%. HR-MS (ESI): m/z 655.1816 (**7**⁺) calcd for C₃₈H₃₈N₂PRu 655.1816.

[CpRu(AsPh₃)(L2)]PF₆ (**8**): Yield: 62%. ¹H NMR (CDCl₃): δ_H = 1.86 (s, 3H, CCH₃), 2.08 (d, ²J_{HH} = 12 Hz, 1H, NCH₂), 2.15 (s, 1H, =CCH₂), 3.73 (s, 1H, =CCH₂), 3.80 (d, ²J_{HH} = 12 Hz, 1H, NCH₂), 4.43 (dd, ²J_{HH} = 16, 48 Hz, 2H, NCH₂), 4.81 (s, 5H, C₅H₅), 6.68 (s, 1H, C_{imi}H), 6.70 (s, 1H, C_{imi}H), 6.85-7.05 (m, 5H, H_{Ph}), 7.18-7.41 (m, 15H, H_{Ph}). ¹³C{¹H} NMR (CDCl₃): δ_C = 30.9 (s, CCH₃), 46.0 (s, =CCH₂), 57.3 (s, NCH₂), 65.8 (s, NCH₂), 79.2.4 (s, =CCH₂), 85.0 (s, C₅H₅), 121.0 (s, C_{imi}H), 122.2 (s, C_{imi}H), 128.2 (s, C_{Ph}), 128.6 (s, C_{Ph}), 129.2 (s, C_{Ph}), 130.7 (s, C_{Ph}), 132.5 (s, C_{Ph}), 134.8 (s, C_{Ph}), 135.4 (s, *ipso* C_{Ph}), 139.4 (s, *ipso* C_{Ph}), 176.1 (s, C-Ru). ³¹P{¹H} NMR (CDCl₃): δ_P = -144.2 (septet, ¹J_{PF} = 713 Hz, PF₆). CHN found (calcd) for [C₃₇H₃₆F₆N₂AsPRu]×0.5CH₃CN: C, 53.35 (53.68), H, 4.58 (4.45), N, 4.24 (4.12)%. HR-MS (ESI): m/z 685.1140 (**8**⁺) calcd for C₃₇H₃₆N₂AsRu 685.1140.

Synthesis of [CpRu(PPh₃)(L1)]₃ (**9**): To a solution of complex **1** (0.36 g, 0.5 mmol) in CH₂Cl₂ (30 mL) was added I₂ crystals (0.26 g, 1 mmol). The resulting mixture was stirred upon which an immediate darkening of the light yellow solution was observed. After 2 hours reaction time, the mixture was concentrated in vacuo, extracted with hexane (3 × 20 mL). The residue was taken up in CH₂Cl₂, passed through a plug of silica, and cooled. Dark yellow crystals formed overnight. Yield: 77%. ¹H NMR ((CD₃)₂CO): δ_H = 1.13 (d, ²J_{HH} = 12 Hz, 1H, NCH₂), 1.74 (s, 3H, CCH₃), 1.89 (d, ³J_{HP} = 15 Hz, 1H, =CCH₂), 2.93 (s, 3H, NCH₃), 3.51 (d, ²J_{HH} = 12 Hz, 1H, NCH₂), 3.75 (s, 1H, =CCH₂), 5.03 (s, 5H, C₅H₅), 6.91 (s, 1H, C_{imi}H), 7.01 (s, 1H, C_{imi}H), 7.22-7.47 (m, 15H, H_{Ph}). ¹³C{¹H} NMR (CD₃CN): δ_C = 32.7 (s, CCH₃), 37.8 (s, NCH₃), 48.1 (s, =CCH₂), 57.5 (s, NCH₂), 81.1 (s, =CCH₂), 88.8 (s, C₅H₅), 118.3 (s, C_{imi}H), 121.4 (s, C_{imi}H), 126.0 (s, C_{Ph}), 129.5 (s, C_{Ph}), 131.4 (s, C_{Ph}), 134.3 (s, *ipso* C_{Ph}), 175.8 (s, C-Ru). ³¹P{¹H} NMR ((CD₃)₂CO): δ_P = 58.1 (s, PPh₃). HR-MS (ESI): m/z 565.1344 (**1**⁺) calcd for C₃₁H₃₂N₂PRu 565.1347.

Transfer hydrogenation catalysis

To a round-bottom flask containing the carbonyl substrate (0.6 mmol), base (1.2 equivalents), anisole (65 μL, 0.6 mmol), and ruthenium complex (2 mol%, 12 μmol) was added 2-propanol (4 mL) and the subsequent reaction mixture was heated under reflux at 110°C for the time indicated. Aliquots (0.05 mL) diluted with CDCl₃ was analysed with ¹H-NMR through which conversions were

determined relative to anisole as the internal standard. All yields are based on the average of at least two runs.

X-ray crystallography of [HL5]Cl, P2, P3, 1, 2, 4, 5, 8, and 9

Single crystal diffraction studies of the compounds were done using Quazar multi-layer optics monochromated Mo K α radiation ($k = 0.71073 \text{ \AA}$) on a Bruker D8 Venture kappa geometry diffractometer with duo μ s sources, a Photon 100 CMOS detector and APEX II control software.²² X-ray diffraction measurements were performed at 150(2) K. Data reduction was performed using SAINT+²² and the intensities were corrected for absorption using SADABS.²² The structures were solved by direct methods using SHELXT,²³ using the SHELXL-2014/7²⁴ program. The non-hydrogen atoms were refined anisotropically. All H atoms were placed in geometrically idealised positions and constrained to ride on their parent atoms. For a table containing the data collection and refinement parameters, see Tables S1-S4 in the Supplementary Information. Crystallographic data for all structures have been deposited with the Cambridge Crystallographic Data Centre (CCDC) as supplementary publication numbers) 1901387 ([HL5]Cl), 1901389 (P3), 1901386 (1), 1901388 (2), 1901385 (4), 1901391 (5), 1901390 (8), and 1901384 (9).

Conflict of interest

There are no conflicts to declare.

Acknowledgements

This work has received support from the South African National Research Foundation (ML Grant nr. 93638 and 115694, FPM Grant nr. 88594) and the Central Research Fund of the University of Pretoria (ML). Selected single crystal X-ray diffraction collections and further assistance by Mr. D. Liles are gratefully acknowledged.

Keywords: ruthenium • N-heterocyclic carbene • transfer hydrogenation • epoxidation • catalysis

References

- (a) Á. Vivancos, C. Segarra, M. Albrecht, *Chem. Rev.* **2018**, *118*, 9493-9586. (b) Y. Wang, L. Duan, L. Wang, H. Chen, J. Sun, L. Sun, M. S. G. Ahlquist, *ACS Catal.* **2015**, *5*, 3966-3972. (c) J. H. Schrittwieser, I. Lavandera, B. Seisser, B. Mautner, J. H. Lutje Spelberg, W. Kroutil, *Tetrahedron: Asymmetry* **2009**, *20*, 483-488.
- (a) D. Wang, D. Astruc, *Chem. Rev.* **2015**, *115*, 6621-6686. (b) R. H. Crabtree, *Chem. Rev.* **2015**, *115*, 127-150. (c) S. Saha, M. Kaur, K. Singh, J. K. Bera, *J. Organomet. Chem.* **2016**, *812*, 87-94.
- (a) F. E. Hahn, A. R. Naziruddin, A. Hepp, T. Pape, *Organometallics* **2010**, *29*, 5283-5288. (b) P. Braunstein, F. Naud, *Angew. Chem. Int. Ed.* **2001**, *40*, 680-699. (c) L. Benhamou, J. Wolf, V. César, A. Labande, R. Poli, N. Lugan, G. Lavigne, *Organometallics* **2009**, *28*, 6981-6993. (d) D. Pugh, A. A. Danopoulos, *Coord. Chem. Rev.* **2007**, *251*, 610-641. (e) F. E. Fernández, M. C. Puerta, P. Valerga,

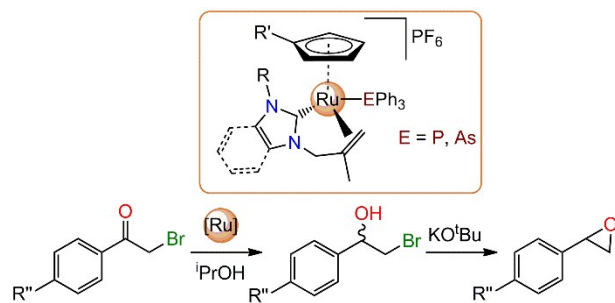
- Inorg. Chem.* **2013**, *52*, 4396-4410. (f) N. Marozsán, H. Horváth, E. Kováts, A. Udvardy, A. Erdei, M. Purgel, F. Joó, *Mol. Catal.* **2018**, *445*, 248-256.
- (a) M. Viciano, M. Feliz, R. Corberán, J. A. Mata, E. Clot, E. Peris, *Organometallics* **2007**, *26*, 5304-5314. (b) S. K. Gupta, J. Choudhury, *Chem. Commun.* **2016**, *52*, 3384-3387. (c) E. Peris, *Chem. Rev.* **2017**, *118*, 9988-10031. (d) V. Leigh, D. J. Carleton, J. Olguin, H. Mueller-Bunz, L. J. Wright, M. Albrecht, *Organometallics* **2014**, *53*, 8054-8060.
- (a) M. J. Bitzer, F. E. Kühn, W. Baratta, *J. Catal.* **2016**, *338*, 222-226. (b) F. Hackenberg, H. Müller-Bunz, R. Smith, W. Streciwilk, X. Zhu, M. Tacke, *Organometallics* **2013**, *32*, 5551-5560. (c) A. Kaiho, H. Suzuki, *Angew. Chem. Int. Ed.* **2012**, *51*, 1408-1411. (d) B. Hildebrandt, C. Ganter, *J. Organomet. Chem.* **2012**, *717*, 83-87. (e) D. Munz, *Organometallics* **2018**, *37*, 275-289.
- (a) J. B. Waters, J. M. Goicoechea, *Coord. Chem. Rev.* **2015**, *293-294*, 80-94. (b) T. Steinke, B. K. Shaw, H. Jong, B. O. Patrick, M. D. Fryzuk, J. C. Green, *J. Am. Chem. Soc.* **2009**, *131*, 10461-10466. (c) C. Gandolfi, M. Heckenroth, A. Neels, G. Laurency, M. Albrecht, *Organometallics* **2009**, *28*, 5112-5121. (d) C. Johnson, M. Albrecht, *Coord. Chem. Rev.* **2017**, *352*, 1-15. (e) R. Pretorius, Z. Mazloomi, Albrecht, M., *J. Organomet. Chem.* **2017**, *845*, 196-205.
- S. Warsink, I. Chang, J. J. Weigend, P. Hauwert, J. Chen, C. J. Elsevier, *Organometallics* **2010**, *29*, 4555-4561.
- D. J. Nielsen, K. J. Cavell, B. W. Skelton, A. H. White, *Organometallics* **2006**, *25*, 4850-4856.
- D. Takaki, T. Okayama, H. Shuto, S. Matsumoto, Y. Yamaguchi, S. Matsumoto, *Dalton Trans.* **2011**, *40*, 1445-1447.
- T. Makino, R. Yamasaki, I. Azumaya, H. Masu, S. Saito, *Organometallics* **2010**, *29*, 6291-6297.
- (a) G. G. Miera, E. Martínez-Castro, B. Martín-Matute, *Organometallics* **2018**, *37*, 636-644. (b) K. Y. Wan, F. Roelfes, A. J. Lough, F. E. Hahn, R. H. Morris, *Organometallics* **2018**, *37*, 491-504.
- (a) F. E. Fernández, M. C. Puerta, P. Valerga, *Organometallics* **2012**, *31*, 6868-6879. (b) Q. Liang, D. Song, *Inorg. Chem.* **2017**, *56*, 11956-11970. (c) Q. Liang, A. Salmon, P. J. Kim, L. Yan, D. Song, *J. Am. Chem. Soc.* **2018**, *140*, 1263-1266. (d) M. F. Lappert, *J. Organomet. Chem.* **1988**, *258*, 185-214.
- (a) V. H. Mai, L. G. Kuzmina, A. V. Churakov, I. Korobkov, J. A. K. Howard, G. I. Nikonov, *Dalton Trans.* **2016**, *45*, 208-215. (b) E. Becker, V. Stingl, G. Dazinger, M. Puchberger, K. Mereiter, K. Kirchner, *J. Am. Chem. Soc.* **2006**, *128*, 6572-6573. (c) D. Schleicher, A. Tronniere, H. Leopold, H. Borrmann, T. Strassner, *Dalton Trans.* **2016**, *45*, 3260-3263. (d) M. Kaloğlu, N. Gürbüz, D. Sémeril, İ. Özdemir, *Eur. J. Inorg. Chem.* **2018**, 1236-1243. (e) W. Li, M. P. Wiesenfeldt, F. Glorius, *J. Am. Chem. Soc.* **2017**, *139*, 2585-2588.
- (a) R. G. Teixeira, A. R. Brása, L. Côte-Real, R. Tatikonda, A. Sanches, M. P. Robalo, F. Avecilla, T. Moreira, M. H. Garcia, M. Haukka, A. Preto, A. Valente, *Eur. J. Med. Chem.* **2018**, *143*, 503-514. (b) V. Miranda-Soto, D. B. Grotjahn, A. L. Cooksy, J. A. Golen, C. E. Moore, A. L. Rheingold, *Angew. Chem. Int. Ed.* **2011**, *50*, 631-635. (c) E. Becker, V. Stingl, G. Dazinger, K. Mereiter, K. Kirchner, *Organometallics* **2007**, *26*, 1531-1535.
- (a) V. W. Truesdale, G. W. Luther, J. E. Greenwood, *Phys. Chem. Chem. Phys.* **2003**, *5*, 3428-3435. (b) J. H. Stern, A. A. Passchier, *J. Phys. Chem.* **1962**, *66*, 752-753. (c) T. Suzuki, *Chem. Rev.* **2011**, *111*, 1825-1845.
- (a) J. DePasquale, M. Kumar, M. Zeller, E. T. Papish, *Organometallics* **2013**, *32*, 966-979. (b) F. E. Fernández, M. C. Puerta, P. Valerga, *Organometallics* **2011**, *30*, 5793-5802. (c) G. I. Nikonov, *Organometallics* **2016**, *35*, 943-949. (d) K. Y. Wan, M. M. H. Syng, A. L. Lough, R. H. Morris, *ACS Catal.* **2017**, *7*, 6827-6842. (e) A. G. Nair, R. T. McBurney, D. B. Walker, M. J. Page, M. R. D. Gatus, M. Bhadbhade, B. A. Messerle, *Dalton Trans.* **2016**, *45*, 14335-14342.
- P. Kumar, R. K. Gupta, D. S. Pandey, *Chem. Soc. Rev.* **2014**, *43*, 707-733.
- M. Hollering, M. Albrecht, F. E. Kühn, *Organometallics* **2016**, *35*, 2980-2986.
- (a) S. Thangavel, S. Boopathi, N. Mahadevaiah, P. Kolaideivel, P. B. Pansuriya, H. B. Friedrich, *J. Mol. Catal. A.* **2016**, *423*, 160-171. (b) R. G. Pearson, *Acc. Chem. Res.* **1993**, *26*, 250-255.
- (a) F. P. Malan, E. Singleton, P. H. van Rooyen, J. Conradie, M. Landman, *New J. Chem.* **2018**, *42*, 19193-19204. (b) R. Fraser, P. H. van Rooyen, J. de Lange, I. Cukrowski, M. Landman, *J. Organomet. Chem.* **2017**, *840*, 11-22. (c) E. V. Gorbachuk, E. K. Badeeva, R. G. Zinnatullin, P. O. Pavlov, A. B. Dobrynin, A. T. Gubaidullin, M. A. Ziganshin, A. V. Gerasimov, O. G. Sinyashin, D. G. Yakhvarov, *J. Organomet. Chem.* **2016**, *805*, 49-53.
- APEX2 (including SAINT and SADABS), Bruker AXS Inc., Madison, WI, **2012**.
- G. M. Sheldrick, *Acta Cryst.* **2015**, *A71*, 3-8.
- G. M. Sheldrick, *Acta Cryst.* **2015**, *C71*, 3-8.

[View Article Online](#)
DOI: 10.1039/C9NJ01220F

New Journal of Chemistry Accepted Manuscript

1
2
3
4
5
6
7
8
9
10
11
12
13
14
15
16
17
18
19
20
21
22
23
24
25
26
27
28
29
30
31
32
33
34
35
36
37
38
39
40
41
42
43
44
45
46
47
48
49
50
51
52
53
54
55
56
57
58
59
60

Graphical abstract



Eight novel alkene-tethered Ru(II)-NHC complexes were employed as catalysts in tandem transfer hydrogenation-epoxidation reactions using phenacyl bromide derivatives as substrates.